



An efficient Ag₂SO₄-deposited ZnO in photocatalytic removal of indigo carmine and phenol under outdoor light irradiation

Hui-Sun Choo^a, Sze-Mun Lam^b, Jin-Chung Sin^c, Abdul Rahman Mohamed^{a,*}

^aSchool of Chemical Engineering, Universiti Sains Malaysia, Engineering Campus, 14300 Nibong Tebal, Pulau Pinang, Malaysia, email: huisun914@gmail.com (H.-S. Choo), Tel. +60 45996410; Fax: +60 45941013; email: chrahman@usm.my (A.R. Mohamed)

^bFaculty of Engineering and Green Technology, Department of Environmental Engineering, Universiti Tunku Abdul Rahman, Jalan Universiti, Bandar Barat, 31900 Kampar, Perak, Malaysia, email: lamsm@utar.edu.my

^cFaculty of Engineering and Green Technology, Department of Petrochemical Engineering, Universiti Tunku Abdul Rahman, Jalan Universiti, Bandar Barat, 31900 Kampar, Perak, Malaysia, email: sinjc@utar.edu.my

Received 11 November 2014; Accepted 9 June 2015

ABSTRACT

Silver sulfate (Ag₂SO₄) was successfully deposited on ZnO via a simple impregnation method. The as-synthesized sample was characterized by X-ray diffraction, scanning electron microscopy, transmission electron microscopy, energy dispersive X-ray spectroscopy, fourier transform infrared spectroscopy, and UV–vis diffuse reflectance spectroscopy. The photocatalytic activities of pure ZnO and 10 wt% Ag₂SO₄/ZnO were evaluated for the removal of indigo carmine and phenol under outdoor light irradiation. The results showed that the photocatalytic activity of Ag₂SO₄/ZnO was higher than those of pure ZnO and commercial TiO₂ for both pollutants removal. Identification of intermediate products and radical scavengers test were also carried out. The effects of process variables such as initial pollutants concentration and solution pH toward the photocatalytic degradation efficiency were also investigated. The optimum initial pollutants concentration was found to be 10 mg/L for both pollutants. The photo removal of indigo carmine was favorable at pH 7 while in the case of phenol, maximum degradation rate was observed at pH 5. The excellent photocatalytic property of Ag₂SO₄-deposited ZnO suggested its potential usage for practical applications in wastewater remediation.

Keywords: Photocatalysis; Silver sulfate; Zinc oxide; Indigo carmine; Phenol

1. Introduction

In the past decades, rapid industrial growth with lack of proper pollution control has led to the environmental damage by variety of organic and inorganic pollutants. Indigo carmine (IC) has been widely employed as colorant in blue jeans textile industry, as additive in pharmaceutical tablets, and capsules as well

as medical diagnostic aid [1,2]. However, due to its highly toxic nature, exposures to indigo carmine will lead to respiratory tract irritation and permanent injury to cornea and conjunctiva [3,4]. Nevertheless, upon its visibility in small quantities, the removal of indigo carmine from wastewater is greatly in need. Similarly, phenol and its derivatives are classified as hazardous components due to their hazard nature and toxicity even at very low concentration. Phenol is mainly being

*Corresponding author.

discharged from petroleum refineries, chemical plants, paper manufacturing industries, and pharmaceutical industries [5,6]. The direct exposures to phenol will cause damage to kidneys, livers, and central nervous system. However, due to the high demand toward these two chemicals, their release into environment through effluent stream is unavoidable. Concerning on these issues, the removal of both pollutants through an efficient and cost-effective way has received extensive attention nowadays. The use of conventional biological treatment is restricted due to their high resistance toward microbial attack [7]. Other pollutants removal method such as membrane ultrafiltration is facing membrane fouling and flux reduction problem. On the other hand, adsorption and coagulation only involved the phase transfer of pollutants from water to another phase which created secondary pollution [8].

In recent years, the introduction of photocatalyst as pollutants removal agent has raised scientist interest as it not only eliminated the hazardous pollutants, but also simultaneously transformed them into non-hazardous components. ZnO has been shown as an effective photocatalyst due to its high photosensitivity, stability, low cost, and non-toxicity properties [9,10]. However, ZnO faced two main drawbacks: (1) large band gap (3.2 eV) that only allowed to response toward UV light irradiation ($\lambda < 380$ nm) and (2) fast recombination of photogenerated electron-hole pairs which limited the photocatalytic activity of ZnO [11,12]. Hence, modification by doping various kinds of metals on ZnO such as Ag, Na, Fe, Co, Cr, Sn, La, Ta, and V on ZnO has been carried out to extend its photo-response into visible light region and to inhibit the recombination of photogenerated electron/hole pair [13]. Nobel metal especially silver (Ag) was found to be a promising metal dopant which can enhance the performance of photocatalyst due to the Schottky barrier formed on Ag-semiconductor interface. Besides, the lower position of Fermi levels and high electron affinity property of silver ion can effectively trap the photogenerated electrons and thus prevented the recombination of photogenerated electron-hole pair [14–16]. However, many Ag/ZnO photocatalysis researches were still limited in using UV-light as energy source [9,17–19]. The introduction of Ag_2SO_4 as dopant in photocatalysis development is rarely reported in literature. The Ag_2SO_4 is foreseen to improve the photocatalytic activity of ZnO due to its high cationic conductivity. Therefore, there is a necessity to carry out a detailed study on the modification of ZnO with Ag_2SO_4 .

In the present study, Ag_2SO_4 was deposited on ZnO via a simple impregnation method which does not involve high temperature and pressure. The

photocatalytic activity of 10 wt% $\text{Ag}_2\text{SO}_4/\text{ZnO}$ was evaluated for the removal of indigo carmine and phenol. The effect of Ag_2SO_4 deposition, initial pollutants concentration, and pH toward pollutants removal were investigated under outdoor light irradiation. Outdoor light was utilized as street light, floodlight, and beacon light. It was safe, movable, and able to provide long lasting light. Moreover, it can establish the similar feature as sunlight which is able to provide artificial solar energy even at night. Hence, the utilization of outdoor lighting as energy source in initiating photocatalysis process would be a safe and environmental friendly option for wastewater remediation.

2. Materials and methodology

2.1. Chemicals

All the chemicals used in this study were of analytical grade without further purification. Zinc nitrate hexahydrate ($\text{Zn}(\text{NO}_3)_2 \cdot 6\text{H}_2\text{O}$) with 98% purity and *p*-benzoquinone (BQ) were obtained from Acros Organic, potassium hydroxide (KOH) with purity 99% and ethanol were purchased from Merck, silver sulfate (Ag_2SO_4) was obtained from BDH, Indigo carmine from nacalai tesque, phenol with 99% purity from Fluka and sodium iodide (NaI) from Hayashi Pure Chemical Industries.

2.2. Synthesis of $\text{Ag}_2\text{SO}_4/\text{ZnO}$

The synthesis of $\text{Ag}_2\text{SO}_4/\text{ZnO}$ was divided into two parts. The pure ZnO particles were prepared according to the method reported in Ref. [20]. To synthesize pure ZnO, the precursor's solution was prepared separately. First, 2 M zinc solution was prepared by dissolving 0.1 mol of zinc nitrate hexahydrate ($\text{Zn}(\text{NO}_3)_2 \cdot 6\text{H}_2\text{O}$) in 50 mL deionized water. Next, 2 M of KOH was added dropwise to the above solution under continuous stirring to adjust the pH of the solution to pH 7. After vigorous stirring for 10 min, the mixture was transferred into Teflon-lined stainless steel autoclaves and heated at 160°C for 18 h. After the reaction completed, the as-prepared precipitate was filtered, washed with deionized water and ethanol, and dried in air at 60°C for 12 h. The doping of Ag_2SO_4 onto ZnO was performed via impregnation method. Briefly, 0.4 g of prepared ZnO was dispersed in 40 mL deionized water. Then, 10 wt% Ag_2SO_4 was added into above solution and the mixture was being continuously stirred for 20 h. After stirring, the as-prepared precipitate was filtered, washed with deionized water for several times, dried in air at 60°C for 12 h, and finally calcined at 300°C in air for 2 h.

2.3. Characterizations

The composition and purity of prepared samples were characterized by X-ray diffraction (XRD) using Philips PW1820 diffractometer equipped with Cu K α radiation. Surface morphology and particle size of prepared samples were analyzed by scanning electron microscope (SEM) via Leo Supra 35Vp-24-58 (supplied by Carl Zeiss, Inc.). Further determination of particle size and shape were done by transmission electron microscopy (TEM) on Philips CM 12 instrument. The functional groups presented in the samples were analyzed by Fourier transform infrared spectroscopy (FTIR) using Thermo Scientific Nicolet iS10 FTIR spectrometer. Diffuse reflectance spectroscopy (DRS) of catalysts was tested in a Perkin Elmer Lambda 35 UV–vis spectrometer.

2.4. Measurement of photocatalytic activities

In this study, indigo carmine and phenol were chosen as model pollutants to examine the photocatalytic activities of pure ZnO and 10 wt% Ag₂SO₄/ZnO. The photocatalytic experiment was performed as follow: 150 mg of catalyst powder was dispersed into 150 mL of 10 mg/L of model pollutant in a 500 mL beaker. Prior to irradiation, the mixture was magnetically stirred for 30 min in dark in order to achieve adsorption–desorption equilibrium of pollutant on the catalyst surface. Then, the mixture was irradiated under outdoor lamp (Philips, 80 W) and bubbled with air at flow rate 7 mL/min. The intensity of light striking on the solution surface was about 11,000 lux, as measured by digital luxmeter. Samples were withdrawn at specific time intervals and filtered twice through 0.02 μ m syringe filter in order to remove the catalyst particles. The change of concentration of indigo carmine at different time intervals was analyzed by UV–vis spectroscopy (Agilent, Cary 60) at maximum wavelength of 609 nm. On the other hand, the concentration of phenol samples were analyzed by high-performance liquid chromatography (HPLC, Perkin Elmer Series 275). The HPLC analysis was performed at 254 nm using mobile phase mixture of water and acetonitrile at ratio 70:30 (v/v) at flow rate of 0.2 mL/min. The total organic carbon (TOC) of degradation of both pollutants was also measured using a Shimadzu TOC-V_{CPH} analyzer to determine the extent of mineralization. The removal efficiency and TOC removal for both pollutants can be obtained by the following equations:

$$\eta(\%) = (C_0 - C)/C_0 \times 100 \quad (1)$$

$$\eta(\%) = (A_0 - A)/A_0 \times 100 \quad (2)$$

$$\text{TOC}(\%) = (\text{TOC}_0 - \text{TOC})/\text{TOC}_0 \times 100 \quad (3)$$

where $\eta(\%)$ and TOC(%) are the pollutant removal efficiency and TOC removal, respectively. C_0 and TOC₀ are the initial concentration, C and TOC are the concentration at specific time, A_0 is the initial absorbance, and A is the absorbance at specific time.

2.5. Detection of active species

In order to examine the role of active species such as hydroxyl radicals ($\cdot\text{OH}$), positive charged hole (h^+) and superoxide anion radicals ($\cdot\text{O}_2^-$) toward the degradation of IC and phenol, different scavengers were used to quench the specific active species. The experimental procedures were similar to the measurement of photocatalytic activity except that 2 mM of different radical scavengers were added into the photocatalytic reaction.

3. Results and discussion

3.1. Characterization

Fig. 1 shows the XRD patterns of pure ZnO and 10 wt% Ag₂SO₄/ZnO. XRD analysis was carried out in order to identify the phase structures of the as-prepared samples. In Fig. 1(a), it can be observed that the diffraction peaks of pure ZnO appeared at 31.8°, 34.4°, 36.3°, 47.5°, 56.6°, 62.8°, 66.3°, 67.8°, 69.0°, 72.5°, and 76.9° which attributed to the crystal plane of ZnO at (1 0 0), (0 0 2), (1 0 1), (1 0 2), (1 1 0), (1 0 3), (2 0 0), (1 1 2), (2 0 1), (0 4 4), and (2 0 2), respectively. The obtained results were in good agreement with the typical hexagonal wurtzite ZnO phase (JCPDS no. 36-1451) [21,22]. No impurity peak was observed in pure ZnO. In addition, the sharp diffraction peak revealed the well crystalline structure of ZnO. Fig. 1(b) is the XRD pattern of 10 wt% Ag₂SO₄/ZnO. The peak at $2\theta = 28.0^\circ, 31.0^\circ, 33.8^\circ, 37.1^\circ$ indicated the presence of silver sulfate (Ag₂SO₄). This verified that Ag₂SO₄ were successfully deposited on ZnO. However, the diffraction peaks for Ag₂SO₄ was not significant. This might be due to the low amount of Ag₂SO₄ deposited on ZnO. Besides, the XRD pattern also showed that the introduction of Ag₂SO₄ on ZnO surface did not change the crystalline structure of ZnO. The average crystalline sizes of the as-prepared catalysts were calculated using the Scherrer equation $D = (0.94\lambda/\beta \cos \theta)$, where D is the crystal size of catalyst, λ is the incident

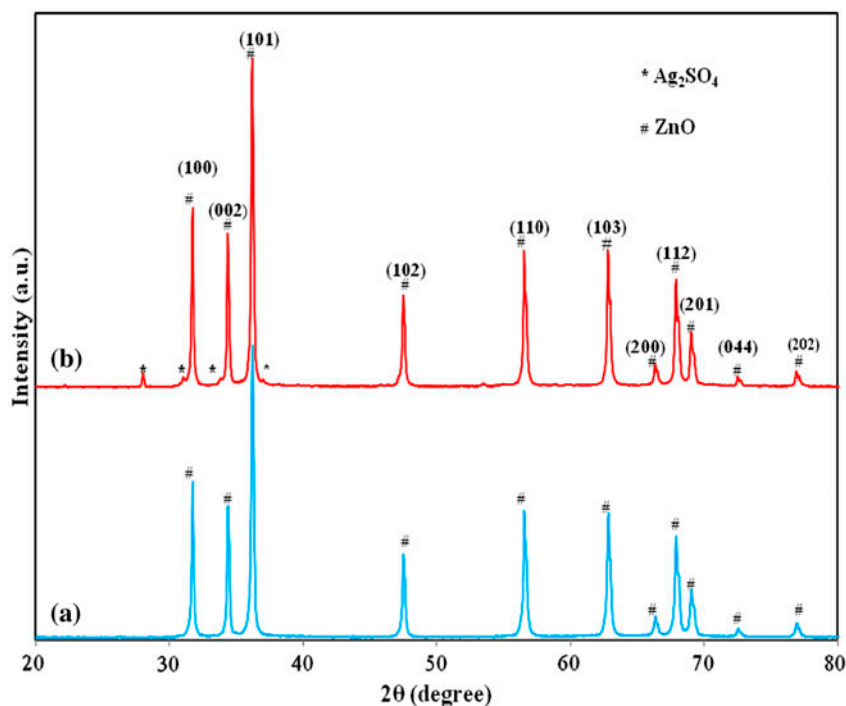


Fig. 1. XRD patterns of (a) pure ZnO and (b) 10 wt% $\text{Ag}_2\text{SO}_4/\text{ZnO}$.

X-ray irradiation, β is the full width at half maximum, and θ is the Bragg angle. The calculated crystalline size of 10 wt% $\text{Ag}_2\text{SO}_4/\text{ZnO}$ was 52.2 nm, which was slightly higher than the pure ZnO (43.5 nm).

Fig. 2(a) and (b) shows the SEM images of pure ZnO and 10 wt% $\text{Ag}_2\text{SO}_4/\text{ZnO}$. Although both images demonstrated agglomeration of particles, each particle boundary remained clearly shown. In addition, the particles were in hexagonal shape with non-uniform sizes. Therefore, it was hard to distinguish ZnO particles and Ag_2SO_4 from the SEM images. Hence, detail particles morphologies were carried out using TEM and the results are shown in Fig. 2(c) and (d). From Fig. 2(c), pure ZnO in hexagonal shape were verified with size ranging 226–260 nm. The shape of ZnO was in agreement with the SEM observation. In addition, clean and smooth surface can be observed on pure ZnO particles. The Fig. 2(d) exhibits the TEM image of 10 wt% $\text{Ag}_2\text{SO}_4/\text{ZnO}$. It was clearly observed that smaller particles of Ag_2SO_4 with sizes about 25–45 nm attached on hexagonal ZnO surface. To further confirm the presence of Ag_2SO_4 on ZnO, the elemental analysis of pure ZnO and 10 wt% $\text{Ag}_2\text{SO}_4/\text{ZnO}$ was also identified using the EDX (Fig. 3). The results confirmed the existence of Zn, O, Ag, and S elements after the modification was done on pure ZnO.

The presence of metal oxide and dopants in as-prepared catalyst were also identified by FTIR analysis. The FTIR spectra of pure ZnO and 10 wt% $\text{Ag}_2\text{SO}_4/\text{ZnO}$ are shown in supplementary material, Fig. S1. Both FTIR spectra were carried out in the range of 400–4,000 cm^{-1} . It can be seen that the main absorption band appeared in the region 440 cm^{-1} for both pure ZnO and 10 wt% $\text{Ag}_2\text{SO}_4/\text{ZnO}$ [23,24]. This strongest absorption peak attributed to the Zn–O bonding which indicated the presence of ZnO in both catalysts. Besides, no significant peak appeared within the region of 500–4,000 cm^{-1} , which demonstrated the high crystalline of ZnO. On the other hand, there were new bands which can be observed after the modification of pure ZnO. By taking a close look on the region of 650–750 cm^{-1} as in the inset of Fig. S1, a new band located at the region of 660 cm^{-1} appeared for 10 wt% $\text{Ag}_2\text{SO}_4/\text{ZnO}$. This absorption peak can be represented in the Ag–O bonding [25]. In addition, there was a mild broad band at 1,100 cm^{-1} which denoted the S–O vibration [26]. The peaks for both Ag–O and S–O band were weak due to the tiny amount of Ag_2SO_4 dopants added, but these two bands once again verified that Ag_2SO_4 had been incorporated into ZnO. While the broad band observed around 3,500 cm^{-1} revealed the occurrences of OH^- on the

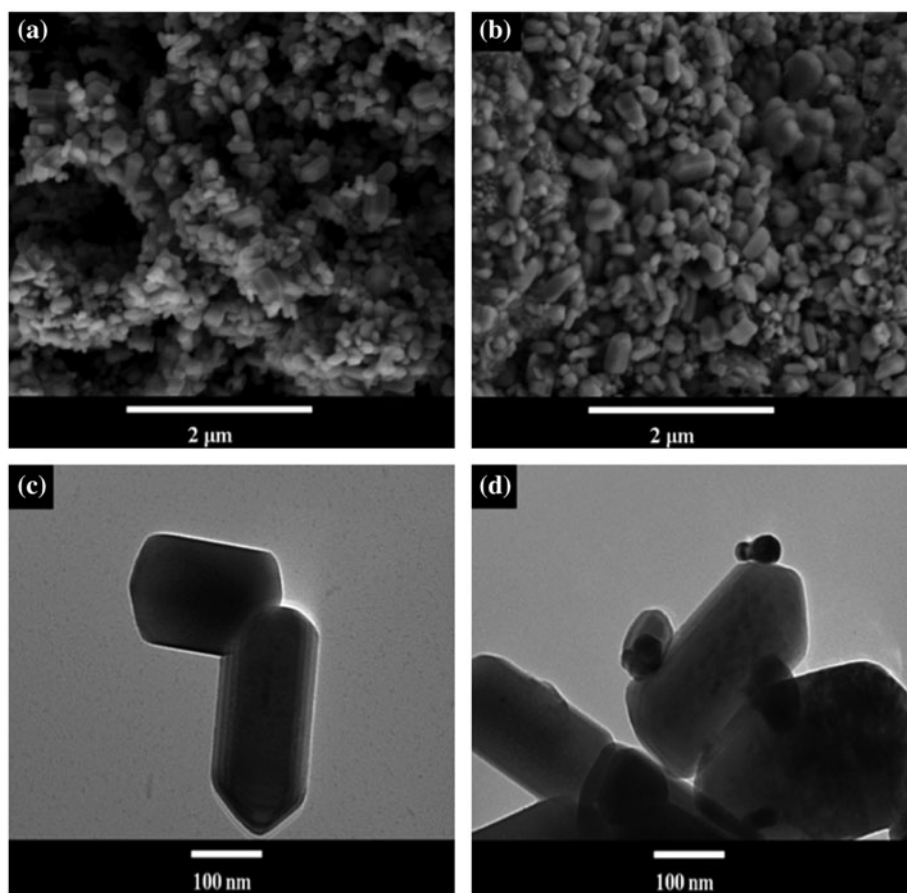


Fig. 2. SEM images of (a) pure ZnO, (b) 10 wt% $\text{Ag}_2\text{SO}_4/\text{ZnO}$; TEM images of (c) pure ZnO, and (d) 10 wt% $\text{Ag}_2\text{SO}_4/\text{ZnO}$.

surface of both catalysts. This might be assigned by the small amount of water molecules adsorbed into the samples during the FTIR analysis.

The UV–vis DRS absorption spectra of pure ZnO as well as 10 wt% $\text{Ag}_2\text{SO}_4/\text{ZnO}$ in the range of 370–700 nm are shown in supplementary material, Fig. S2. It was clearly demonstrated that the band gap absorption of both catalysts were around 400–410 nm. The absorption edge of pure ZnO was at 406 nm while for 10 wt% $\text{Ag}_2\text{SO}_4/\text{ZnO}$ was at 401 nm. Hence, the band gap energies could be calculated using the formula below [27]:

$$E_g = hc/\lambda = 1240/\lambda \quad (4)$$

where E_g represents the band gap energy (eV), h is the plank's constant (4.135677×10^{-15} eVs), c is the velocity of light (3×10^8 m/s), and λ represents the wavelength (nm) of adsorption edge. By using the formula in Eq. (4), the band gap energies were calculated to be 3.05 and 3.09 eV for pure ZnO and 10 wt% $\text{Ag}_2\text{SO}_4/\text{ZnO}$,

respectively. A slight blue shift of 10 wt% $\text{Ag}_2\text{SO}_4/\text{ZnO}$ was observed compared to pure ZnO. However, 10 wt% $\text{Ag}_2\text{SO}_4/\text{ZnO}$ showed stronger absorption band in the range of 400–700 nm compared to pure ZnO. This revealed that the introduction of Ag_2SO_4 on ZnO can strongly enhance the visible light absorption which led to the generation of more electron–hole pairs under visible light irradiation. According to Ahmed et al. [14], the increase of visible light absorption was due to the changing of dielectric constant of ZnO surrounding matrix caused by Ag_2SO_4 doping. Thus, absorption property deduced that the 10 wt% $\text{Ag}_2\text{SO}_4/\text{ZnO}$ could be promising in solar photocatalysis.

3.2. Photocatalytic activity of $\text{Ag}_2\text{SO}_4/\text{ZnO}$

The photocatalytic activities of the $\text{Ag}_2\text{SO}_4/\text{ZnO}$ were evaluated for the removal of IC and phenol under outdoor light illumination. The results are shown in Fig. 4. Photolysis and darkness adsorption

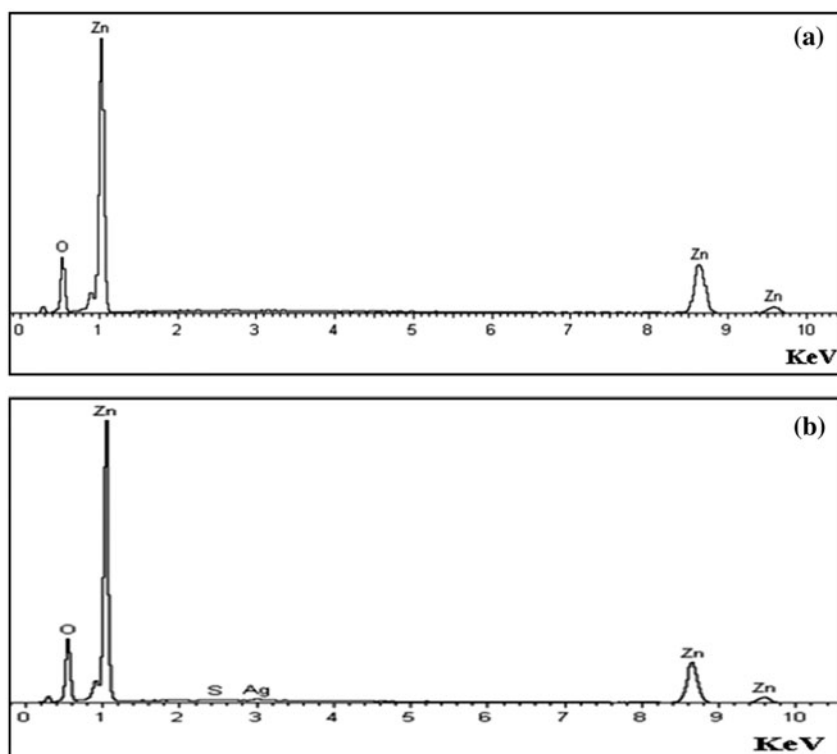


Fig. 3. EDX of (a) pure ZnO and (b) 10 wt% $\text{Ag}_2\text{SO}_4/\text{ZnO}$.

tests were also carried out as control experiments. In the case of IC removal, the decolorization efficiencies were almost negligible in both control experiments. This indicated that the presence of catalyst and light played essential roles in initiating the photocatalytic removal of IC. In Fig. 4(a), the results also indicated that the photocatalytic activity of ZnO was greatly improved after impregnated with Ag_2SO_4 . After 20 min irradiation, 97.8% of IC removal was achieved by 10 wt% $\text{Ag}_2\text{SO}_4/\text{ZnO}$, which was 4.7 times higher than commercial TiO_2 and 7.2 times higher than pure ZnO. The performance of 10 wt% $\text{Ag}_2\text{SO}_4/\text{ZnO}$ can also be observed from the UV–vis absorbance spectra profiles of the IC solution collected at different time intervals as shown in Fig. 4(b). The peak at 609 nm which was the maximum peak of IC gradually reduced and nearly disappeared after 20 min irradiation. This indicated that almost complete removal of IC had been achieved. The suggested degradation pathway of IC was displayed in supplementary material, Fig. S3. Basically, rupturing the chromophore group of IC will lead to the decolorization of IC. The active species presented in the reaction will first break the C–C bond and C–N bond of the chromophore group into various kinds of intermediate products. The intermediate products formed including aromatic

intermediates such as anthranilic acid, nitrobenzaldehyde, and nitrobenzene, and aliphatic acids such as fumaric acid. The continuous attacking of active species will induce ring opening to form aliphatic acids and eventually degraded to end products which were CO_2 , NO_3^- and SO_4^{2-} . Since the intermediate products in the photocatalytic degradation of IC was not identified in this study, the degradation pathway drawn by Vautier et al. [28] was proposed in our system.

On the other hand, Fig. 4(c) demonstrated the degradation of phenol in photolysis and darkness adsorption tests was extremely low. Besides, it can be observed that the 10 wt% $\text{Ag}_2\text{SO}_4/\text{ZnO}$ showed the highest phenol degradation efficiency (98.7%), which once again revealed the modification of ZnO by Ag_2SO_4 can effectively improve the photocatalytic activity of ZnO. The degradation efficiency of 10 wt% $\text{Ag}_2\text{SO}_4/\text{ZnO}$ was 1.3 times higher than pure ZnO and 2.7 times higher than commercial TiO_2 . The time-dependent HPLC profiles of phenol solution displayed in Fig. 4(d) clearly showed that the phenol peak appeared at retention time (RT) 5.7 min gradually decreased with the increasing of reaction time. This indicated the superior photocatalytic activity of 10 wt% $\text{Ag}_2\text{SO}_4/\text{ZnO}$. In addition to the above-mentioned main compound, the peaks at RT 1.1 and 3.3 min

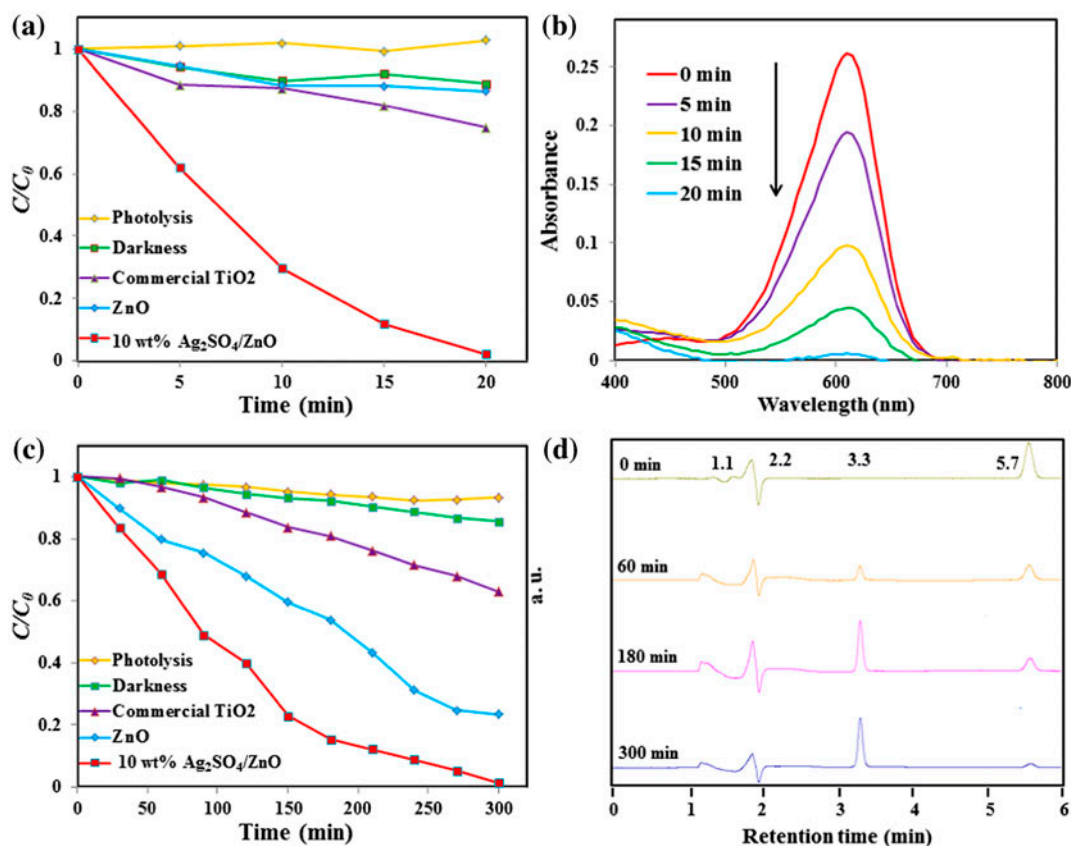


Fig. 4. (a) Photocatalytic performance of Ag_2SO_4 deposited ZnO with various Ag_2SO_4 content in IC solution, (b) UV-vis absorbance spectra of IC solution in the presence of 10 wt% $\text{Ag}_2\text{SO}_4/\text{ZnO}$ at difference time interval, (c) photocatalytic performance of Ag_2SO_4 deposited ZnO with various Ag_2SO_4 content in phenol solution, and (d) HPLC profile of phenol degradation by 10 wt% $\text{Ag}_2\text{SO}_4/\text{ZnO}$ at different time interval. (Amount of catalyst: 1 g/L, concentration of pollutant: 10 mg/L, air flow rate: 7 mL/min, pH 7 (IC); 5 (phenol)).

could be assigned to muconic acid and benzoquinone intermediates, respectively, when compared with the standard chemicals. This identification was in agreement with that reported in our previous studies [29,30]. The suggested degradation pathway of phenol is shown in supplementary material, Fig. S4. The attack of active species toward phenol led to the formation of aromatic intermediate product such as hydroquinone. It should also be noted that the benzoquinone would be generated due to dehydrogenation reaction of hydroquinone [31]. These aromatic intermediates would undergo ring cleavage reaction to yield aliphatic acids such as muconic acid, which would eventually convert to CO_2 and H_2O due to decarboxylation [32].

3.3. Effect of initial pollutant concentration

The effect of initial pollutant concentration toward the photocatalytic removal efficiency was investigated

and the results are shown in Fig. 5. The examined range of initial concentrations varied from 10 to 50 mg/L for IC removal, while 10 to 40 mg/L for phenol degradation. The results clearly showed that the removal efficiencies for both pollutants decreased with the increasing of the initial pollutant concentration. Therefore, it can be concluded that the highest removal rate for both pollutants was 10 mg/L.

Two presumed factors could hinder the degradation of both pollutants when their initial concentration was high. Firstly, the increased amount of 2,4-DCP may occupy a greater number of active sites of photocatalysts, which then suppressed generation of the active species and resulted in a lower removal rate [18,33,34]. Secondly, with the increase in the pollutant concentration, the photons absorbed by the pollutants were more than that of photocatalyst [35,36]. Consequently, fewer photons managed to activate the photocatalyst surface essentially decreased the removal efficiency of the catalysts when high concentrated pollutant was used.

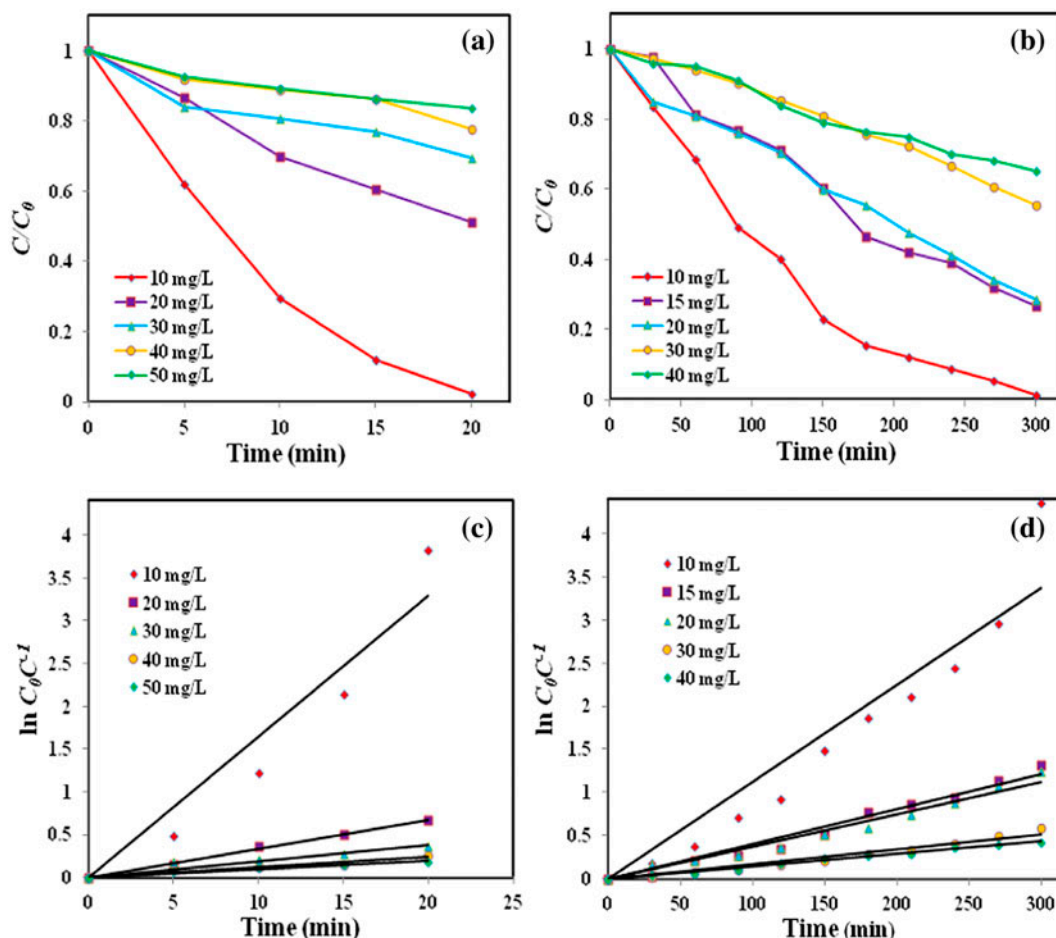


Fig. 5. (a) Effect of initial IC concentration on the photocatalytic decolorization of IC, (b) effect of initial phenol concentration on the photocatalytic degradation of phenol, (c) kinetics study of photocatalytic removal of IC for different initial concentration by 10 wt% $\text{Ag}_2\text{SO}_4/\text{ZnO}$, and (d) kinetics study of photocatalytic degradation of phenol for different initial concentration by 10 wt% $\text{Ag}_2\text{SO}_4/\text{ZnO}$. (Catalyst: 10 wt% $\text{Ag}_2\text{SO}_4/\text{ZnO}$, amount of catalyst: 1 g/L, air flow rate: 7 mL/min, pH 7 (IC); 5 (phenol)).

3.4. Kinetic study

Since initial pollutant concentration has significant influence on the pollutant degradation rate, kinetic studies of photocatalytic removal of different initial pollutant concentrations were calculated and displayed in Fig. 5(c) and (d). The obtained straight lines revealed that the photocatalytic reaction obeyed pseudo-first-order kinetics according to Langmuir–Hinselwood (L–H) kinetic model which could be expressed in Eq. (5) [37]:

$$d[C]/dt = k_{\text{app}}[C] \quad (5)$$

where k_{app} is the apparent pseudo-first-order rate constant. The integration of Eq. (5) will give Eq. (6).

$$\ln(C_0/C) = k_{\text{app}}t \quad (6)$$

where C_0 refers to initial pollutant concentration, C is the pollutant concentration at specific time, k_{app} is apparent rate constant, and t refers to time (min).

The calculated apparent rate constant (k_{app}) of different initial concentrations of IC and phenol are shown in Table 1. The k_{app} value decreased with the increase of initial pollutant concentration and maximum value was obtained at 10 mg/L for both pollutants.

3.5. Effect of initial pH

It was crucial to study the effect of initial pH as it played an important role in pollutant removal efficiency. In this study, the pH solution for both pollutants

was varied from range 3.0–9.0 by adjustment of hydrochloric acid (HCl) and sodium hydroxide (NaOH). The natural pH was determined to be 7.0 for IC and 5.0 for phenol. Fig. 6 illustrates the removal efficiencies of IC and phenol as a function of solution pH. From Fig. 6(a), the removal efficiency of IC increased with increase in solution pH from pH 3.0 to 7.0, while the removal efficiency dropped with further increase in solution pH to 9.0. In the case of phenol as depicted in Fig. 6(b), the maximum degradation was attained at pH 5.0. This was in line with the results reported by few available studies [38,39].

It was known that pH of solution affected the adsorption of pollutant molecules on ZnO surface. The point of zero charge (pH_{zpc}) of ZnO was reported to be 8.6 [40]. When the solution pH was lower than pH_{zpc} , the catalyst surface acquired a net positive charge; hence IC anionic dye and phenol molecules could easily adsorb on the surface of ZnO due to the electrostatic attraction. It was interesting to note that the removal for both pollutants reached optimum at their natural pH. At high acidic condition (pH 3), the solution was adjusted by HCl, the presence of Cl^- anions in acidic solution might lead to the competition between pollutant molecules, and Cl^- anions for the adsorption of active site on ZnO surface, thus decreased the photocatalytic activity of 10 wt% Ag_2SO_4/ZnO [41]. However, at natural pH, the solution did not acquire any pH adjustment, hence Cl^- anions did not exist. In the absence of Cl^- anions in solution, maximum adsorption of anionic dye molecules and phenol molecules on 10 wt% Ag_2SO_4/ZnO surface were achieved and led to the high removal efficiency of both pollutants.

On the contrary, at higher pH, the surface of 10 wt% Ag_2SO_4/ZnO was in negatively charge. The electrostatic repulsion between 10 wt% Ag_2SO_4/ZnO with anionic indigo carmine dye and phenolate anions caused the poor adsorption of pollutant molecules onto the surface of photocatalyst. This led to the low pollutants removal efficiency. Moreover, the alkaline

solution was adjusted with NaOH. The competition of Na^+ and OH^- ions with the pollutant molecules for the adsorption sites on catalyst surface can also lead to lower photocatalytic activity [42].

3.6. Mineralization of IC and phenol

In order to investigate the mineralization extent of IC and phenol over 10 wt% Ag_2SO_4/ZnO , the irradiated solution also analyzed by TOC. The results of TOC removal for both pollutants are displayed in Fig. 7. It showed that the TOC concentration decreased gradually with reaction time as the pollutants removed. This verified the progressive mineralization of pollutants resulting from an effective decomposition of aromatic intermediates. After 20 min irradiation, 66% of TOC removal was observed with the removal of IC. In the case of phenol, maximum TOC removal was observed at 70% after 300 min irradiation. The slight difference between the TOC and degradation percentage revealed the existence of incomplete mineralized organic carbon in the pollutant solutions [43].

3.7. Role of active species

The role of active species was carried out by performing the radical scavengers test. Different radical scavengers were loaded into the photocatalytic reaction in order to quench the specific active species. In this study, ethanol was employed as $\cdot OH$ scavenger in the photocatalysis reaction [29], sodium iodide (NaI) was chosen to quench h^+ [43], while *p*-benzoquinone (BQ) was introduced as $\cdot O_2^-$ scavenger [44]. The effects of these scavengers toward the pollutants degradation are shown in Fig. 8.

As can be seen, the photocatalytic degradation of both pollutants was greatly suppressed in the presence of scavengers. The extent of decrease in the degradation efficiency that induced by the scavenger, indicating the importance of the corresponding active species. Hence, these results suggested that hole and

Table 1

The value of apparent rate constant (k_{app}) and correlation coefficient (R^2) at different initial pollutants concentrations

Initial pollutants concentration (mg L ⁻¹)	k_{app} (min ⁻¹)		R^2	
	IC	Phenol	IC	Phenol
10	0.1641	0.6743	0.9238	0.9120
20	0.0337	0.2427	0.9957	0.9670
30	0.0190	0.2254	0.9000	0.9702
40	0.0118	0.1026	0.9448	0.9510
50	0.0097	0.0858	0.9322	0.9858

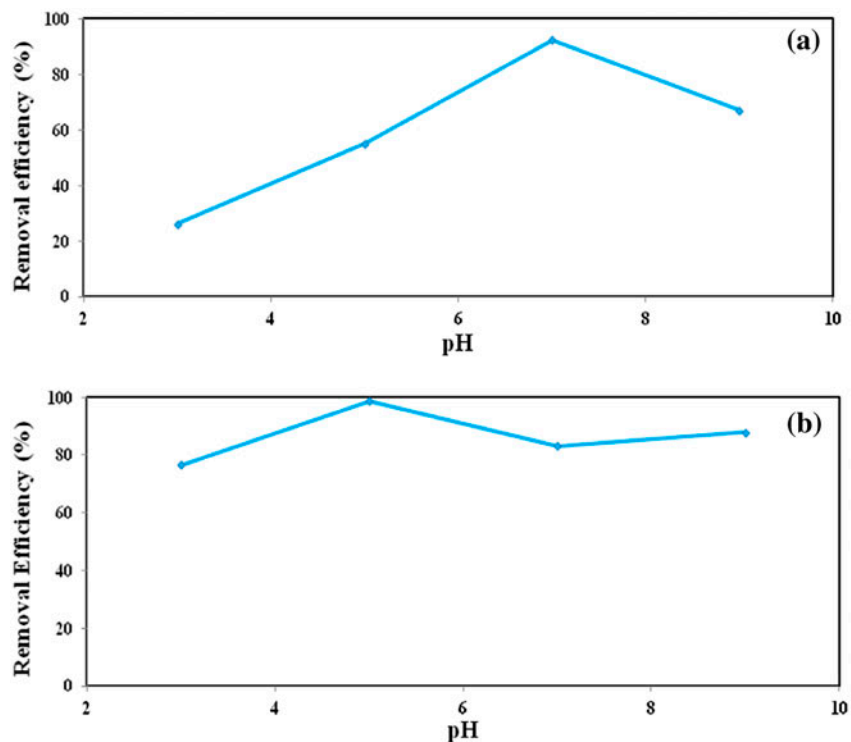


Fig. 6. (a) Effect of solution pH on the photocatalytic removal of IC, and (b) effect of solution pH on the photocatalytic degradation of phenol. (Catalyst: 10 wt% $\text{Ag}_2\text{SO}_4/\text{ZnO}$, amount of catalyst: 1 g/L, concentration of pollutants: 10 mg/L, air flow rate: 7 mL/min).

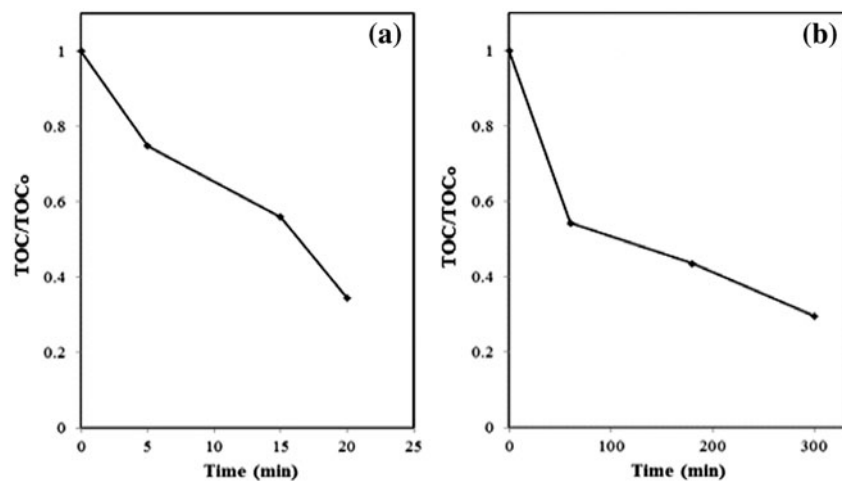


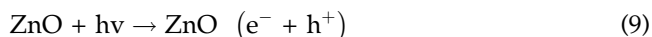
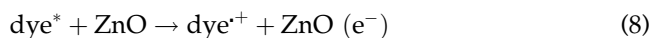
Fig. 7. TOC removal of (a) indigo carmine, and (b) phenol over 10 wt% $\text{Ag}_2\text{SO}_4/\text{ZnO}$ (amount of catalyst: 1 g/L, concentration of pollutant: 10 mg/L, air flow rate: 7 mL/min, pH 7 (IC); 5 (phenol)).

$\cdot\text{O}_2^-$ were the main active species responsible in degradation of IC. In the case of phenol, hole, $\cdot\text{O}_2^-$ and $\cdot\text{OH}$ were the main active species contributed in degradation of phenol. The results obtained were in line with other studies as well [45,46].

3.8. Mechanism study for photocatalytic removal of IC and phenol

Fig. 9(a) illustrates the mechanism scheme proposed for the photocatalytic decolorization of IC.

Dye had self-sensitized properties under visible light irradiation, which is known as photosensitized effect [42,47]. When sufficient photon energy is provided, the adsorbed dye pollutants are excited (dye^*). The photo-generated electron (e^-) will be injected to the conduction band (CB) of ZnO. At the mean time, ZnO also received sufficient photon energy that will promote the excited e^- from valance band (VB) to CB of ZnO, leaving holes (h^+) behind. According to few available studies [48,49], Ag_2SO_4 can receive e^- and reduced to Ag. The presence of Ag on ZnO can effectively trap the e^- from CB of ZnO to inhibit the recombination of photo-generated electron–hole pairs. The trapped e^- was then transferred to the surface and reacted with the oxygen molecules (O_2) to form reactive superoxide radical anions ($\text{O}_2^{\cdot-}$). The $\text{O}_2^{\cdot-}$ can undergo a series of reaction and converted to $\cdot\text{OH}$ radicals. On the contrary, the h^+ in VB of ZnO can receive e^- from hydroxyl ions (OH^-), water molecules (H_2O) and sulfate anions (SO_4^{2-}) which dissociated from Ag_2SO_4 , generating reactive $\cdot\text{OH}$ and $\text{SO}_4^{\cdot-}$ radicals. The dye^* which lost e^- were extremely unstable and easily degraded upon reacted with highly reactive $\cdot\text{OH}$ and $\text{SO}_4^{\cdot-}$ radicals. The mechanism of IC decolorization for $\text{Ag}_2\text{SO}_4/\text{ZnO}$ can be summarized as below [50–53]:



On the other hand, the mechanism for the photocatalytic degradation of phenol is slightly different from photocatalytic removal of IC as phenol does not have self-sensitized properties as shown in Fig. 9(b). The mechanism of the charge transfer for phenol degradation can refer to Eqs. (9)–(17). The Ag deposited in the ZnO surface which reduced from Ag_2SO_4 can act as a good electron sink and promoted the interfacial charge-transfer between Ag and ZnO. At the same time, the h^+ leaving behind can accept e^- from OH^- , H_2O and SO_4^{2-} generating $\cdot\text{OH}$ and $\text{SO}_4^{\cdot-}$ radicals. Thus, continual charge transfer and rapid separation of e^- – h^+ pairs enhanced the yield of highly reactive species in the degradation of pollutants, which further improved the photocatalytic activity of $\text{Ag}_2\text{SO}_4/\text{ZnO}$.

4. Conclusion

In summary, $\text{Ag}_2\text{SO}_4/\text{ZnO}$ was successfully synthesized by a simple impregnation method and confirmed by XRD, SEM, TEM, EDX, FTIR, and UV–vis DRS measurements. The photocatalytic activity of $\text{Ag}_2\text{SO}_4/\text{ZnO}$ was tested in IC and phenol removal under irradiation of outdoor light. The $\text{Ag}_2\text{SO}_4/\text{ZnO}$ exhibited superior pollutant removal efficiencies compared to pure ZnO and commercial TiO_2 . The high photocatalytic performance of $\text{Ag}_2\text{SO}_4/\text{ZnO}$ was due to the cooperative role between photo-reduced Ag and ZnO enhanced the separation of photogenerated

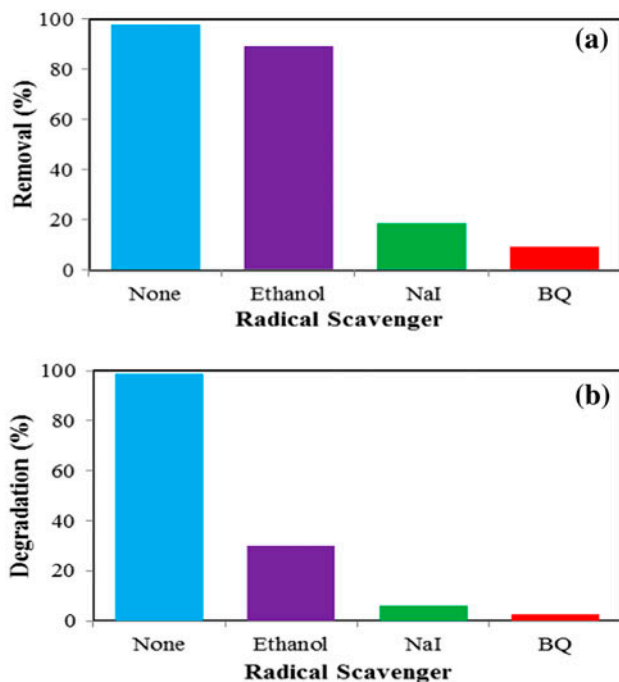


Fig. 8. Effect of various radical scavengers toward the photocatalytic removal of (a) indigo carmine, and (b) phenol over 10 wt% $\text{Ag}_2\text{SO}_4/\text{ZnO}$. (Amount of catalyst: 1 g/L, concentration of pollutant: 10 mg/L, air flow rate: 7 mL/min, pH 7 (IC); 5 (phenol)).

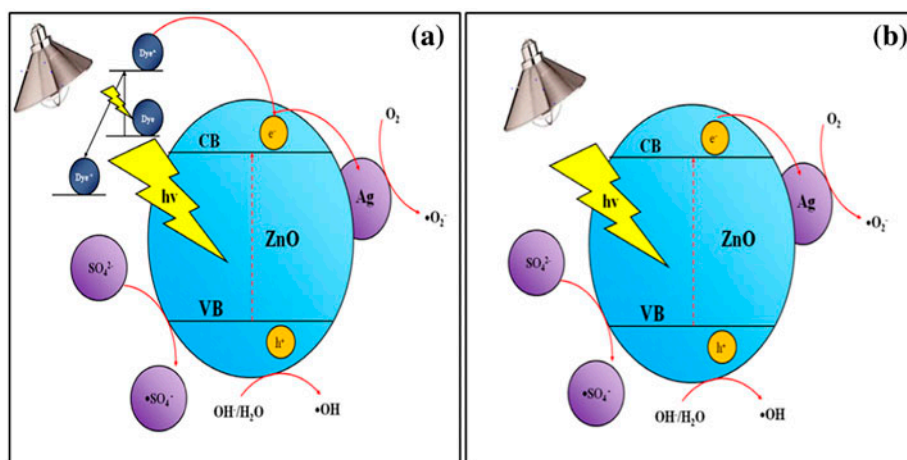


Fig. 9. Proposed mechanism for photocatalytic removal of (a) IC and (b) phenol by $\text{Ag}_2\text{SO}_4/\text{ZnO}$ under outdoor light irradiation.

electron–hole pair. The investigation of photocatalytic ability also showed that the $\text{Ag}_2\text{SO}_4/\text{ZnO}$ was affected by initial pollutant concentration and solution pH. High degradation of both pollutants was observed at initial pollutant concentration of 10 mg/L and at natural pH. Furthermore, the as-synthesized $\text{Ag}_2\text{SO}_4/\text{ZnO}$ also exhibited a high mineralization capacity of IC and phenol. Hence, $\text{Ag}_2\text{SO}_4/\text{ZnO}$ could be a potential photocatalyst applied in wastewater remediation and environmental protection.

Supplementary material

The supplementary material for this paper is available online at <http://dx.doi.org/10.1080/19443994.2015.1067833>.

Acknowledgement

This research was supported by Research Universiti Grant (No. 814176) and International Research Collaboration Fund (No. 910404) from Universiti Sains Malaysia and MyBrain 15 scholarship through Malaysia Government.

References

- [1] U.R. Lakshmi, V.C. Srivastava, I.D. Mall, D.H. Lataye, Rice husk ash as an effective adsorbent: Evaluation of adsorptive characteristics for Indigo Carmine dye, *J. Environ. Manage.* 90 (2009) 710–720.
- [2] A. Bentouami, M.S. Ouali, L.C. De-Menorval, Photocatalytic decolourization of indigo carmine on 1,10-phenanthroline intercalated bentonite under UV-B and solar irradiation, *J. Photochem. Photobiol. A: Chem.* 212 (2010) 101–106.
- [3] A. Mittal, J. Mittal, L. Kurup, Batch and bulk removal of hazardous dye, indigo carmine from wastewater through adsorption, *J. Hazard. Mater.* 137 (2006) 591–602.
- [4] M.S. Secula, I. Crețescu, S. Petrescu, An experimental study of indigo carmine removal from aqueous solution by electrocoagulation, *Desalination* 277 (2011) 227–235.
- [5] Y.F. Zhang, R. Selvaraj, M. Sillanpää, Y.H. Kim, C.W. Tai, The influence of operating parameters on heterogeneous photocatalytic mineralization of phenol over BiPO_4 , *Chem. Eng. J.* 245 (2014) 117–123.
- [6] B.C. Meikap, G.K. Rot, Removal of phenolic compound from industrial waste water by semi fluidized bed bio-reactor, *J. IPHE India* 3 (2007) 54–61.
- [7] C.P. Sajan, B. Basavalingu, S. Ananda, K. Byrappa, Comparative study on the photodegradation of Indigo Carmine dye using commercial TiO_2 and natural rutile, *J. Geol. Soc. India* 77 (2011) 82–88.
- [8] U.G. Akpan, B.H. Hameed, Parameters affecting the photocatalytic degradation of dyes using TiO_2 -based photocatalysts: A review, *J. Hazard. Mater.* 170 (2009) 520–529.
- [9] B. Subash, B. Krishnakumar, M. Swaminathan, M. Shanthi, Enhanced photocatalytic performance of WO_3 loaded Ag–ZnO for Acid Black 1 degradation by UV-A light, *J. Mol. Catal. A: Chem.* 366 (2013) 54–63.
- [10] S. Sakthivel, B. Neppolian, M.V. Shankar, B. Arabindoo, M. Palanichamy, V. Murugesan, Solar photocatalytic degradation of azo dye: Comparison of photocatalytic efficiency of ZnO and TiO_2 , *Sol. Energy Mater. Sol. Cells* 77 (2003) 65–82.
- [11] Y. Zhou, S.X. Lu, W.G. Xu, Photocatalytic activity of Nd-doped ZnO for the degradation of C.I. reactive blue 4 in aqueous suspension, *Environ. Prog. Sustainable Energy* 28 (2009) 226–233.
- [12] J.H. Sun, L.P. Qiao, S.P. Sun, G.L. Wang, Photocatalytic degradation of Orange G on nitrogen-doped

- TiO₂ catalysts under visible light and sunlight irradiation, *J. Hazard. Mater.* 155 (2008) 312–319.
- [13] J.H. Sun, S.Y. Dong, J.L. Feng, X.J. Yin, X.C. Zhao, Enhanced sunlight photocatalytic performance of Sn-doped ZnO for Methylene Blue degradation, *J. Mol. Catal. A: Chem.* 335 (2011) 145–150.
- [14] S. Ahmed, M.G. Rasul, R. Brown, M.A. Hashib, Influence of parameters on the heterogeneous photocatalytic degradation of pesticides and phenolic contaminants in wastewater: A short review, *J. Environ. Manage.* 92 (2011) 311–330.
- [15] H. Liu, X.N. Dong, G.J. Li, X. Su, Z.F. Zhu, Synthesis of C, Ag co-modified TiO₂ photocatalyst and its application in waste water purification, *Appl. Surf. Sci.* 271 (2013) 276–283.
- [16] B. Divband, M. Khatamian, G.R.K. Eslamian, M. Darbandi, Synthesis of Ag/ZnO nanostructures by different methods and investigation of their photocatalytic efficiency for 4-nitrophenol degradation, *Appl. Surf. Sci.* 284 (2013) 80–86.
- [17] A. Meng, S.B. Sun, Z.J. Li, J.K. Han, Synthesis, characterization, and dispersion behavior of ZnO/Ag nanocomposites, *Adv. Powder Technol.* 24 (2013) 224–228.
- [18] A. Senthilraja, B. Subash, B. Krishnakumar, D. Rajamanickam, M. Swaminathan, M. Shanthi, Synthesis, characterization and catalytic activity of co-doped Ag–Au–ZnO for MB dye degradation under UV-A light, *Mater. Sci. Semicond. Process.* 22 (2014) 83–91.
- [19] H.Q. Bian, S.Y. Ma, Z.M. Zhang, J.M. Gao, H.B. Zhu, Microstructure and Raman scattering of Ag-doping ZnO films deposited on buffer layers, *J. Cryst. Growth* 394 (2014) 132–136.
- [20] N. Kiomarsipour, R.S. Shoja Razavi, Hydrothermal synthesis and optical property of scale and spindle-like ZnO, *Ceram. Int.* 39 (2013) 813–818.
- [21] J.C. Sin, S.M. Lam, I. Satoshi, K.T. Lee, A.R. Mohamed, Sunlight photocatalytic activity enhancement and mechanism of novel europium-doped ZnO hierarchical micro/nanospheres for degradation of phenol, *Appl. Catal. B: Environ.* 148–149 (2014) 258–268.
- [22] T.G. Venkatesha, Y.A. Arthoba Nayaka, R. Viswanatha, C.C. Vidyasagar, B.K. Chethana, Electrochemical synthesis and photocatalytic behavior of flower shaped ZnO microstructures, *Powder Technol.* 225 (2012) 232–238.
- [23] T. Parvin, N. Keerthiraj, I.A. Ibrahim, S. Phanichphant, K. Byrappa, Photocatalytic degradation of municipal wastewater and brilliant blue dye using hydrothermally synthesized surface-modified silver-doped ZnO designer particles, *Int. J. Photoenergy* 2012 (2012) 670610.
- [24] V. Srivastava, D. Gusain, Y.C. Sharma, Synthesis, characterization and application of zinc oxide nanoparticles (n-ZnO), *Ceram. Int.* 39 (2013) 9803–9808.
- [25] K. Namratha, S. Suresha, M.B. Nayan, K. Byrappa, Synthesis, characterization, and photocatalytic properties of surface modified silver doped ZnO, *Res. Chem. Intermed.* 37 (2011) 531–539.
- [26] C.R. Martins, G. Ruggeri, M.A. De-Paoli, Synthesis in pilot plant scale and physical properties of sulfonated polystyrene, *J. Braz. Chem. Soc.* 14 (2003) 797–802.
- [27] J. He, Q.Z. Cai, D. Zhu, Q. Luo, D.Q. Zhang, X.W. Li, In-situ preparation of WO₃/TiO₂ composite film with increased photo quantum efficiency on titanium substrate, *Curr. Appl. Phys.* 11 (2011) 98–100.
- [28] M. Vautier, C. Guillard, J.M. Herrmann, Photocatalytic degradation of dyes in water: Case study of indigo and of indigo carmine, *J. Catal.* 201 (2001) 46–59.
- [29] J.C. Sin, S.M. Lam, K.T. Lee, A.R. Mohamed, Self-assembly fabrication of ZnO hierarchical micro/nanospheres for enhanced photocatalytic degradation of endocrine-disrupting chemicals, *Mater. Sci. Semicond. Process.* 16 (2013) 1542–1550.
- [30] S.M. Lam, J.C. Sin, A.Z. Abdullah, A.R. Mohamed, Efficient photodegradation of endocrine-disrupting chemicals with Bi₂O₃–ZnO nanorods under a compact fluorescent lamp, *Water Air Soil Pollut.* 224 (2013) 1565.
- [31] J.C. Sin, S.M. Lam, K.T. Lee, A.R. Mohamed, Preparation and photocatalytic properties of visible light-driven samarium-doped ZnO nanorods, *Ceram. Int.* 39 (2013) 5833–5843.
- [32] S.M. Lam, J.C. Sin, I. Satoshi, A.Z. Abdullah, A.R. Mohamed, Enhanced sunlight photocatalytic performance over Nb₂O₅/ZnO nanorod composites and the mechanism study, *Appl. Catal. A: Gen.* 471 (2014) 126–135.
- [33] A.P. Toor, A. Verma, C.K. Jotshi, P.K. Bajpai, V. Singh, Photocatalytic degradation of Direct Yellow 12 dye using UV/TiO₂ in a shallow pond slurry reactor, *Dyes Pigm.* 68 (2006) 53–60.
- [34] F.D. Mai, C.C. Chen, J.L. Chen, S.C. Liu, Photodegradation of methyl green using visible irradiation in ZnO suspensions, *J. Chromatogr. A* 1189 (2008) 355–365.
- [35] N. Daneshvar, M.H. Rasoulifard, A.R. Khataee, F. Hosseinzadeh, Removal of C.I. Acid Orange 7 from aqueous solution by UV irradiation in the presence of ZnO nanopowder, *J. Hazard. Mater.* 143 (2007) 95–101.
- [36] B. Krishnakumar, B. Subash, M. Swaminathan, AgBr–ZnO—An efficient nano-photocatalyst for the mineralization of Acid Black 1 with UV light, *Sep. Purif. Technol.* 85 (2012) 35–44.
- [37] B. Subash, B. Krishnakumar, V. Pandiyan, M. Swaminathan, M. Shanthi, An efficient nanostructured Ag₂S–ZnO for degradation of Acid Black 1 dye under day light illumination, *Sep. Purif. Technol.* 96 (2012) 204–213.
- [38] S.K. Pardeshi, A.B. Patil, A simple route for photocatalytic degradation of phenol in aqueous zinc oxide suspension using solar energy, *Solar Energy* 82 (2008) 700–705.
- [39] S.G. Anju, S. Yesodharan, E.P. Yesodharan, Zinc oxide mediated sonophotocatalytic degradation of phenol in water, *Chem. Eng. J.* 189–190 (2012) 84–93.
- [40] H. Benhebal, M. Chaib, T.S. Geens, A. Leonard, S.D. Lambert, M. Crine, B. Heinrichs, Photocatalytic degradation of phenol and benzoic acid using zinc oxide powders prepared by the sol–gel process, *AEJ* 52 (2013) 517–523.
- [41] S.M. Lam, J.C. Sin, A.R. Mohamed, Parameter effect on photocatalytic degradation of phenol using TiO₂-P25/activated carbon (AC), *Korean J. Chem. Eng.* 27 (2010) 1109–1116.
- [42] S.M. Lam, J.C. Sin, A.Z. Abdullah, A.R. Mohamed, Degradation of wastewaters containing organic dyes photocatalysed by zinc oxide: A review, *Desalin. Water Treat.* 41 (2012) 131–169.

- [43] J.C. Sin, S.M. Lam, K.T. Lee, A.R. Mohamed, Photocatalytic performance of novel samarium-doped spherical-like ZnO hierarchical nanostructures under visible light irradiation for 2,4-dichlorophenol degradation, *J. Colloid Interface Sci.* 401 (2013) 40–49.
- [44] P.F. Ji, J.L. Zhang, F. Chen, M. Anpo, Study of adsorption and degradation of acid orange 7 on the surface of CeO₂ under visible light irradiation, *Appl. Catal. B: Environ.* 85 (2009) 148–154.
- [45] Y.X. Chen, S.Y. Yang, K. Wang, L.P. Lou, Role of primary active species and TiO₂ surface characteristic in UV-illuminated photodegradation of Acid Orange 7, *J. Photochem. Photobiol. A: Chem.* 172 (2005) 47–54.
- [46] X.W. Zhang, D.D. Sun, G.T. Li, Y.Z. Wang, Investigation of the roles of active oxygen species in photodegradation of azo dye AO7 in TiO₂ photocatalysis illuminated by microwave electrodeless lamp, *J. Photochem. Photobiol. A: Chem.* 199 (2008) 311–315.
- [47] J.F. Guo, J.X. Li, A.Y. Yin, K.N. Fan, W.L. Dai, Photodegradation of Rhodamine B on sulfur doped ZnO/TiO₂ nanocomposite photocatalyst under visible-light irradiation, *Chin. J. Chem.* 28 (2010) 2144–2150.
- [48] T. Kawai, T. Sakata, *New Horizons in Catalysis: Part 7B*, Elsevier Scientific Publishing Company, Amsterdam, 1981.
- [49] A. Tanaka, Y. Nishino, S. Sakaguchi, T. Yoshikawa, K. Imamura, K. Hashimoto, H. Kominami, Functionalization of a plasmonic Au/TiO₂ photocatalyst with an Ag co-catalyst for quantitative reduction of nitrobenzene to aniline in 2-propanol suspensions under irradiation of visible light, *Chem. Commun.* 49 (2013) 2551–2553.
- [50] R.L. Qiu, D.D. Zhang, Y.Q. Mo, L. Song, E. Brewer, X.F. Huang, Y. Xiong, Photocatalytic activity of polymer-modified ZnO under visible light irradiation, *J. Hazard. Mater.* 156 (2008) 80–85.
- [51] W.R. Cao, L.F. Chen, Z.W. Qi, Highly dispersed Ag₂SO₄ nanoparticles deposited on ZnO nanoflakes as photocatalysts, *Catal. Lett.* 144 (2014) 598–606.
- [52] B.B. Zermeno, E. Moctezuma, R.G. Alamilia, Photocatalytic degradation phenol and 4-chlorophenol with titania, oxygen and ozone, *Sustainable Environ. Res.* 21 (2011) 299–305.
- [53] Z.J. Zhang, W.Z. Wang, M. Shang, W.Z. Yin, Photocatalytic degradation of Rhodamine B and phenol by solution combustion synthesized BiVO₄ photocatalyst, *Catal. Commun.* 11 (2010) 982–986.